

## COUNTING ALGORITHM FOR SEQUENTIAL OPTICAL IMAGES OF IMMUNOREACTIVE MOUSE TASTE BUD CELLS

KATSUMI TATENO<sup>1</sup>, OSAMU SHIKU<sup>2</sup> AND YOSHITAKA OHTUBO<sup>1</sup>

<sup>1</sup>Department of Human Intelligence Systems  
Kyushu Institute of Technology  
2-4, Hibikino, Wakamatsu-ku, Kitakyushu-shi, Fukuoka 808-0196, Japan  
{tateno; otsubo}@brain.kyutech.ac.jp

<sup>2</sup>Department of Control Engineering  
National Institute of Technology, Sasebo College  
1-1, Okishin-cho, Sasebo city, Nagasaki 857-1193, Japan  
shiku@sasebo.ac.jp

Received July 2019; accepted October 2019

**ABSTRACT.** *We developed a counting algorithm for use with sequential optical images of immunoreactive mouse taste bud cells. To count the immunoreactive cells in serial thin sections, continuity of a cell through the sequential sections must be confirmed. For this purpose, we used the overlap ratio of the cell regions in given sections and the distance between the sections. Results show that the mean positive predictive value for mouse taste bud cells was 99%; the mean sensitivity was 73%. Gamma correction improved the mean sensitivity to 87% with a slight decrease in the mean positive predictive value (94%).*

**Keywords:** Taste bud cells, Fluorescence image, Image processing, Confocal microscope

**1. Introduction.** Immunohistostaining based on an antigen-antibody reaction is a conventional method used to investigate the expression of specific molecules such as proteins and their developmental changes in cells and tissues [1,2]. After preparations are immunohistostained, the distribution of antibodies labeled with a fluorescent dye against the specific molecules (antigen) is visualized using a confocal microscope by which sequential optical images can be acquired from the bottom to top of tissues. Under a confocal laser-scanning microscope, cells have a three-dimensional structure in tissues. Consequently, for quantitative analysis of the expression of specific molecules, researchers should count the immunoreactive cells in the sequential optical images. In general, cell images in the sequential optical images are segmented from image noise by experts [1,2]. Therefore, cell counting is a time-consuming job.

Figure 1(a) depicts a schematic diagram of a vertical cross-section of a single taste bud in peeled epithelia of mouse. Several dozens of taste cells are tightly packed in a single taste bud. In fact, it is hard to identify an isolated cell in a 3-dimensional reconstructed image of G $\gamma$ 13-immunoreactive cells in a single taste bud (Figure 1(b)).

Algorithms for the segmentation of cells in a two-dimensional image are effective for counting cells on a dish [3,4]. Those algorithms are useful to count cells on each transversal slice of sequential optical images. For three dimensions, continuity of the segmented cells along the vertical axis is a concern. A confocal microscope is well-suited for 3D imaging of biological tissues in vivo. Forero and his coworkers have reported automatic counting methods for nervous systems of *Drosophila* [5-8]. They used 18-connectivity between slices of the vertical direction. The minimum volume is a key parameter to identify the cell.

An optical section (ultrathin section) in sequential optical images generally has thickness that is less than the diameter of an immunoreactive cell. Therefore, the same cell

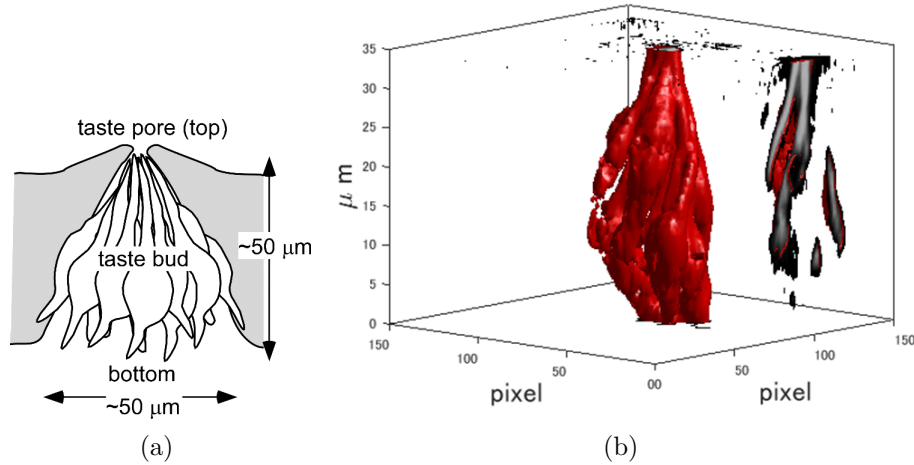


FIGURE 1. (color online) (a) Schematic diagram of a vertical cross-section of a single taste bud in peeled epithelia. A single taste bud contains 50 elongated taste bud cells which are classified into three cell types, (b) three-dimensional reconstructed image of  $G\gamma 13$ -immunoreactive cells in a single taste bud. These surfaces were reconstructed by a MATLAB function, isosurface.

might be found through several sections. For counting the immunoreactive cell, the continuity of the cell must be detected in addition to the segmentation of the cell image in each section. The continuity of cell images must be considered along with the segmentation of a cell image in each section. This study was conducted to develop an algorithm for the automatic counting of immunoreactive cells in serial ultrathin sections.

## 2. Methods.

**2.1. Immunohistostaining of taste bud cells and acquisition of sequential optical images.** Sequential optical images were obtained from peeled epithelia containing taste buds in mouse soft palates, as described previously [1,9]. Briefly, the peeled soft palate epithelia were fixed with 4% paraformaldehyde in phosphate-buffered saline (PBS). They were immunohistostained with primary antibodies immunoreactive to  $G\gamma 13$  (a G-protein  $\gamma$  subunit, anti- $G\gamma 13$  goat polyclonal antibody, 1 : 100 dilution) and  $IP_3R3$  (an  $IP_3$  receptor subtype, anti- $IP_3R3$  mouse monoclonal antibody, 1 : 50) for 24-48 h at 4°C. After washing the epithelia with PBS, we incubated them with the Alexa Fluor-conjugated secondary antibodies, Alexa 555-conjugated donkey anti-mouse IgG (1 : 400), and Alexa 633-conjugated donkey anti-goat IgG (1 : 200), for 24-48 h at 4°C.

The stained preparations were investigated using a confocal microscope (TCS-SL, Leica Microsystems, Germany). Optical section images were obtained from the entire length of the taste buds with sequential acquisition in 1.0  $\mu\text{m}$  steps. We scanned each focal plane three times and used the averaged images for analysis. We applied the proposed counting algorithm to the five taste buds (TB1-5) obtained.

For control experiments, we used software (Scion Image ver.  $\beta 4.03$ ; Scion Corp., USA) to count the soma of immunoreactive cells manually, as the number of immunoreactive cells per taste bud. We pursued the soma of taste bud cells as an immunohistostained ring through a series of optical slices (original image in Figure 2). When the ring appeared on at least five continuous images, we identified it as soma.

To estimate the minimum distance of soma between two taste bud cells in the vertical direction, we stained the cell nuclei with acridine orange (a fluorescent dye for nucleus stain), acquired sequential optical images from whole taste buds in 1.0  $\mu\text{m}$  steps by the confocal microscopy, and then measured the length of the nucleus. The lengths of the

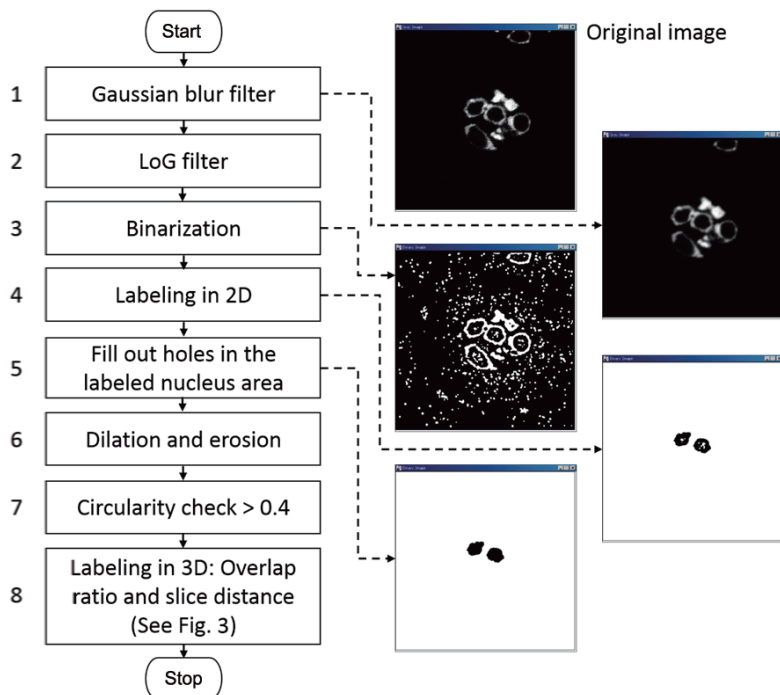


FIGURE 2. Block diagram showing the proposed image processing algorithm and the filtered images

obtained nuclei were  $7.5 \pm 2.3 \mu\text{m}$  (mean  $\pm$  S.D.,  $n = 1945$ ). Because the distance of the center of soma between two taste bud cells is at least ca.  $5 \mu\text{m}$ , the center of cells should not be close mutually less than  $5 \mu\text{m}$ . Therefore, we assume that  $5 \mu\text{m}$  (five sequential optical slices) and greater are necessary to distinguish cells from each other distributed in a vertical direction.

**2.2. Counting algorithms.** Gray image files of sequential thin sections of mouse taste bud cells were prepared. The image size is  $512 \times 512$  pixels ( $60 \times 60 \mu\text{m}$ ). The resolution is 8 bits. Five taste bud cells were used. Each set of image files included  $G\gamma 13$ -immunoreactive or  $IP_3R3$ -immunoreactive cells.

Figure 2 portrays a flowchart of the image processing procedure and detailed descriptions of the steps as follows. 1) A Gaussian blur filter is applied to images to reduce image noise and detailed information. We expected to blur the edge of the cell image. The filter size is  $13 \times 13$  pixels. 2) The Laplacian of Gaussian (LoG) filter is applied to the images. The filter size is  $13 \times 13$  pixels. 3) The filtered images are converted to binary images. The pixel is assigned to black if the LoG response is positive. Otherwise, the pixel is assigned to white. 4) The related component labeling is applied to the binary image in two dimensions. North and West neighbors of the pixel were used for the connectivity check. It is four-connectivity. The labeled area is added to a list of a possible cell nucleus if the labeled area is greater than 500 pixels and the width or height is less than 300 pixels. 5) A hole in the labeled area is filled out if the hole is smaller than 400 pixels. 6) Dilation and erosion of the binary image are repeated twice to suppress the background noise. 7) The circularity of the labeled nucleus area is calculated. Finally, we segmented the cell nucleus which met the following conditions: the circularity is greater than 0.4; the pixel number of the labeled area is greater than 500 pixels; either the width or height is less than 300 pixels. 8) An overlap ratio of the labeled nucleus area in the given two sections is calculated (Figure 3(a)). A square circumscribed around the labeled nucleus area ( $S_A$  and  $S_B$ ) and the overlap area  $S_0$  is calculated. The overlap ratios  $k_A = S_0/S_A$  and  $k_B = S_0/S_B$  are calculated. The two labeled nucleus areas are regarded as the same

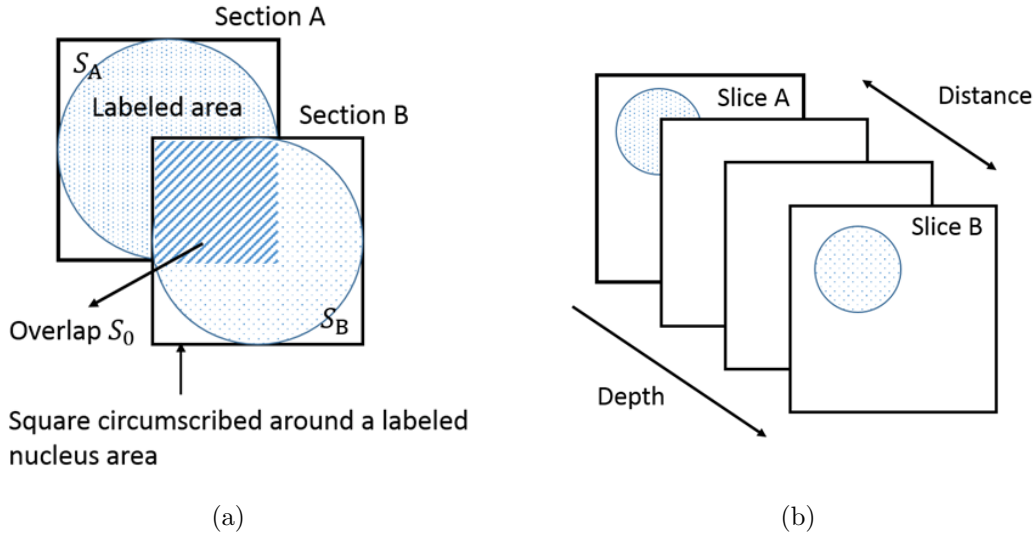


FIGURE 3. Three-dimensional continuity of a cell: a) overlap ratio, b) maximum length limitation of a nucleus

cell if the overlap ratio  $k_A$  or  $k_B$  is greater than 0.8 and if the given two sections exist within a distance of four sections (Figure 3(b)), meaning that the nucleus length is less than  $5 \mu\text{m}$ .

**2.3. Assessment of the proposed counting algorithm.** The results were classified into three categories as follows: true positive (TP) – a cell was located where an expert found an immunoreactive cell; false positive (FP) – a cell was located incorrectly where an immunoreactive cell was absent; and false negative (FN) – a cell was absent where an expert found an immunoreactive cell. Sensitivity and the positive predictive value (PV+) were defined respectively as  $TP/(TP + FN)$  and  $TP/(TP + FP)$ .

**3. Results.** Elongated taste bud cells are classified into three cell types, type I, II, and III cells [10,11]. Type II cells are taste receptor cells which express umami, sweet, and bitter G protein-coupled receptors and signal transduction-related proteins [12-14]. Therefore, it is important for understanding taste signal transduction at a cellular level to clarify the proportion of type II cells per a taste bud. In this experiment, we used type II cell markers,  $G\gamma 13$  or  $IP_3R3$ , to count type II cells in a single taste bud. Immunoreactivity for a  $G\gamma 13$  antibody was observed through entire taste buds as shown in Figure 4. Also, we observed the same results using the  $IP_3R3$  antibody. We counted the soma of type II cell markers (immunohistostained rings) as the number of type II cells per a single taste bud (see Methods section).

Labeled nuclei (pseudo-colored green in Figure 4) are superimposed on  $G\gamma 13$  images in Figure 4. At most 2 nuclei were labeled in a section. Three-dimensional surfaces of the labeled nuclei were reconstructed by a MATLAB function, isosurface. 9 chunks of nuclei were found in Figure 5. If nuclei are found in sequential sections, the isosurface function reconstructed smooth surfaces. If our proposed algorithm fails to label an existing nucleus, isolated chunks are displayed in 3D isosurface reconstruction. In fact, a right top barrel (filled triangle in Figure 5) and a disk (triangle in Figure 5) are derived from the same cell. Their distance was separated by  $2 \mu\text{m}$ . As the separation was less than  $5 \mu\text{m}$  and those labeled nuclei were well overlapped, the proposed algorithm regarded the indicated barrel and disk as the same cell.

We used sequential optical images from the taste pore to the bottom of the taste buds. The taste bud boundary is determined by an expert in the transversal section of differential

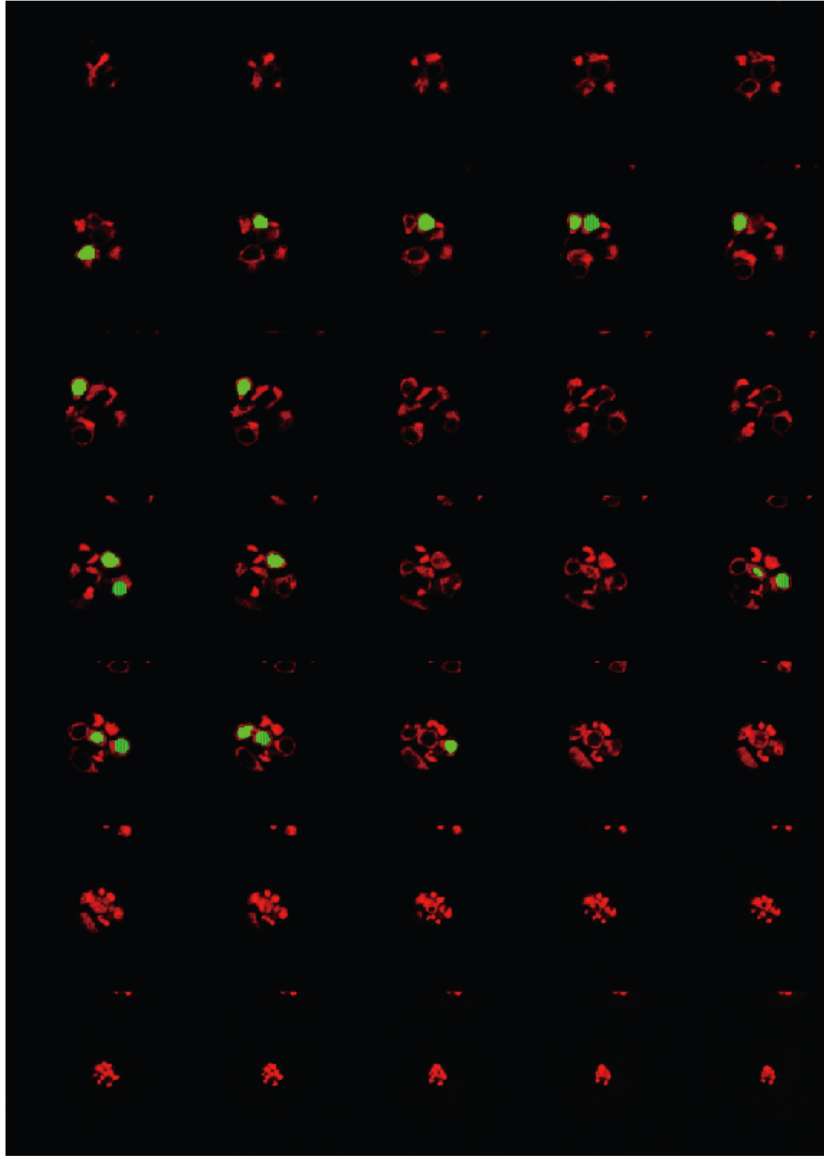


FIGURE 4. (color online) Sequential confocal images obtained from a single taste bud (pseudo-colored red) and detected nucleus area (pseudo-colored green). Sequential images of immunoreactivity to  $G\gamma 13$  are showed from bottom (upper left) to top (lower right) of a taste bud with  $1.0 \mu\text{m}$  optical steps.

interference contrast microscope imaging. Figure 6 presents results of segmentation for  $G\gamma 13$ -immunoreactive cells or  $IP_3R3$ -immunoreactive cells obtained using the proposed counting algorithm. The results were compared with the cell images identified by an expert (Figures 6(b) and 6(d)). In the  $G\gamma 13$ -immunoreactive cell image, 8 cells were detected in the boundary of respective taste buds. An expert found 11 cells. The locations of the identified cell overlapped the figure drawn by the expert. Undetected taste bud cells were three. Although the expert expected that the taste bud cell lies concealed, the counting algorithm did not detect it.

Results of the counting algorithms for  $G\gamma 13$ -immunoreactive cells are presented in Table 1. There is no FP for all taste buds, but there are 30% undetected taste bud cells (FN). Especially, numerous taste bud cells were undetected in TB3 and TB5. The mean PV+ was 1.0 for all taste buds. The sensitivity was approximately 0.7.

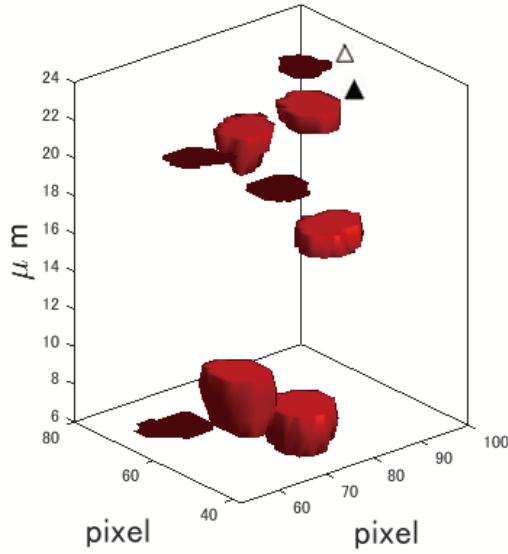


FIGURE 5. (color online) 3D reconstructed nuclei. Barrel-shaped 9 chunks are detected. Top right barrel (filled triangle) and a disk (triangle) are derived from the same taste bud cell.

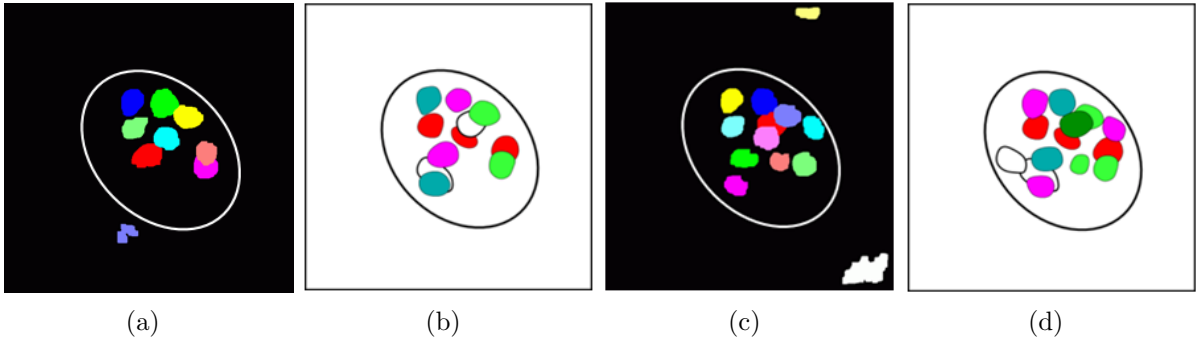


FIGURE 6. (color online) Segmented  $G\gamma 13$ - ((a) and (b)) and  $IP_3R3$ - ((c) and (d)) immunoreactive cells in a taste bud. (a) and (c) segmentation by the proposed counting algorithm. (b) and (d) cell images identified by an expert. It is noteworthy that circles roughly represent the boundary of respective taste buds. All identified cells are displayed on the same plane.

TABLE 1. Counting results of  $G\gamma 13$ -immunoreactive cells

	TB1	TB2	TB3	TB4	TB5	Mean
True positive	8	12	20	14	12	
False positive	0	0	0	0	0	
False negative	3	5	10	3	9	
Sensitivity	0.73	0.71	0.67	0.82	0.57	0.7
PV+	1.0	1.0	1.0	1.0	1.0	1.0

Many of the taste bud cells are immunoreactive to  $IP_3R3$  (Table 2). There are few FPs. Results show that 24% of the taste bud cells were undetected. The mean PV+ was 0.98 for all taste buds. The mean sensitivity was about 0.76. This sensitivity is better than those shown in results obtained for  $G\gamma 13$ -immunoreactive cells.

To improve sensitivity, the gamma value of the images was tuned. Table 3 presents the gamma dependence of the mean sensitivity and mean PV+ value. For tuning the

TABLE 2. Counting results of IP<sub>3</sub>R3-immunoreactive cells

	TB1	TB2	TB3	TB4	TB5	Mean
True positive	11	14	26	19	18	
False positive	0	0	1	0	1	
False negative	3	5	10	3	9	
Sensitivity	0.79	0.74	0.72	0.86	0.67	0.76
PV+	1.0	1.0	0.96	1.0	0.95	0.98

TABLE 3. Gamma value correction

	Gamma value	1	1.5	2.0	2.5	3.0
G <sub>γ13</sub>	Mean sensitivity	0.7	0.75	0.84	0.88	0.93
	Mean PV+	1.0	0.97	0.95	0.9	0.86
IP <sub>3</sub> R3	Mean sensitivity	0.76	0.86	0.91	0.91	0.94
	Mean PV+	0.98	0.98	0.94	0.93	0.92

gamma value, the number of undetected taste buds was reduced. The mean sensitivity was improved with a slight decrease in the mean positive predictive value.

The counting algorithm was implemented in C language. The present processing time information was based on a Ubuntu Linux PC with Core 2 processors (1.86 GHz). This counting algorithm required 10 to 20 seconds for each taste bud. For an expert, the counting of taste bud cells through sequential optical images takes several minutes. Therefore, the expert saves time for the quantitative analysis by using this algorithm.

**4. Conclusions.** The present counting algorithm counts cells in immunoreactive mouse taste bud cells. For the continuity check, we infer that a high overlap ratio and the fraction of a cell in one slice is found in another near slice. If the distance between the segmented cells is five sections (= 5  $\mu\text{m}$ ) or more, then those are regarded as different cells in the present algorithm. The nucleus is roughly 9  $\mu\text{m}$  long. The current assumption corresponds to a half of the longitudinal length of the nucleus because the present algorithm detects a cell at the thick part of the cell nucleus.

This counting algorithm is applicable to sequential optical images of other immunoreactive cells. For application of the counting algorithm to other immunoreactive cells, the dimensions of the nucleus size and the minimum distance between cells should be suitably selected.

## REFERENCES

- [1] Y. Ohtubo and K. Yoshii, Quantitative analysis of taste bud cell numbers in fungiform and soft palate taste buds of mice, *Brain Res.*, vol.1367, pp.13-21, 2011.
- [2] Y. Ohtubo, M. Iwamoto and K. Yoshii, Subtype-dependent postnatal development of taste receptor cells in mouse fungiform taste buds, *Eur. J. Neurosci.*, vol.35, no.11, pp.1661-1671, 2012.
- [3] H. Refai, L. Li, T. K. Teague and R. Naukam, Automatic count of hepatocytes in microscopic images, *Proc. of 2003 Int. Conf. Image Process.*, vol.2, pp.1101-1104, 2003.
- [4] Y. Ma, R. Dai, L. Lian and Z. Zhang, An counting and segmentation method of blood cell image with logical and morphological feature of cell, *Chinese J. Electron.*, vol.11, no.1, pp.53-55, 2002.
- [5] M. G. Forero, J. A. Pennack, A. R. Learte and A. Hidalgo, DeadEasy caspase: Automatic counting of apoptotic cells in Drosophila, *PLoS One*, vol.4, no.5, 2009.
- [6] M. G. Forero, A. R. Learte, S. Cartwright and A. Hidalgo, DeadEasy mito-glia: Automatic counting of mitotic cells and glial cells in Drosophila, *PLoS One*, vol.5, no.5, 2010.
- [7] M. G. Forero, J. A. Pennack and A. Hidalgo, DeadEasy neurons: Automatic counting of HB9 neuronal nuclei in Drosophila, *Cytom. Part A*, vol.77, no.4, pp.371-378, 2010.
- [8] M. G. Forero, K. Kato and A. Hidalgo, Automatic cell counting in vivo in the larval nervous system of Drosophila, *J. Microsc.*, vol.246, no.2, pp.202-212, 2012.

- [9] T. Noguchi, Y. Ikeda, M. Miyajima and K. Yoshii, Voltage-gated channels involved in taste responses and characterizing taste bud cells in mouse soft palates, *Brain Res.*, vol.982, no.2, pp.241-259, 2003.
- [10] R. G. Murray, The ultrastructure of taste buds, in *The Ultrastructure of Sensory Organs*, I. Friedmann (ed.), Amsterdam, North-Holland Publishing Company, 1973.
- [11] S. D. Roper, Taste buds as peripheral chemosensory processors, *Semin Cell Dev Biol.*, vol.24, no.1, pp.71-79, 2013.
- [12] E. Adler, M. A. Hoon, K. L. Mueller, J. Chandrashekar, N. J. Ryba and C. S. Zuker, A novel family of mammalian taste receptors, *Cell*, vol.100, pp.693-702, 2000.
- [13] G. Nelson, J. Chandrashekar, M. A. Hoon, L. Feng, G. Zhao, N. J. Ryba and C. S. Zuker, An amino-acid taste receptor, *Nature*, vol.416, pp.199-202, 2002.
- [14] T. R. Clapp, R. Yang, C. L. Stoick, S. C. Kinnamon and J. C. Kinnamon, Morphologic characterization of rat taste receptor cells that express components of the phospholipase C signaling pathway, *J. Comp. Neurol.*, vol.468, pp.311-321, 2004.